Title

Energy Performance of Zeolite-Based Drying Bead Desiccants Used to Dry Paddy Rice.

Journal
ACS Omega, 9(36)

Authors
Ying, Tianyu
Dien, Alice
Kornbluth, Kurt
et al.

Publication Date
2024-09-10

DOI
10.1021/acsomega.4c04153

Peer reviewed

ACS OMEGA

http://pubs.acs.org/journal/acsodf
Article

Energy Performance of Zeolite-Based Drying Bead Desiccants Used to Dry Paddy Rice

Tianyu Ying, Alice Dien, Kurt Kornbluth, Christopher W Simmons, Irwin R. Donis-González,* and Edward S. Spang*

Cite This: *ACS Omega* 2024, 9, 38142−38152
Read Online

ABSTRACT: This study utilizes differential scanning calorimetry and thermogravimetric analysis to assess the total energy required to regenerate saturated zeolite-based drying beads (DBs) used to dry paddy rice. We quantify the required heat energy for DB regeneration by calculating the area under the curve in a heat flow rate versus time graph, with the end of the regeneration process indicated by stabilization of the DB weight. Our findings suggest that at DB regeneration temperatures ranging from 120 to 350 °C, the process varied from 813 to 22 min, demonstrating that higher temperatures lead to faster regeneration speeds. The total energy used for regeneration showed similar values at 250 and 350 °C, averaging around 2032 and 2136 kJ per kg of dried DB, respectively. Additionally, the study showed that DBs can hold water between 28.7% and 54.4% higher than the manufacturer's specifications, suggesting a reduced quantity of DBs required for effective paddy rice drying. The overall required heat energy for the regeneration process was calculated at 4.86 MJ/kg, with a carbon intensity of approximately 275.61 g of CO_2-eq per kg of water removed, resulting in lower values compared to conventional drying methods. The study underscores DB's possibility of lower total energy (thermal and electrical) consumption and greenhouse gas emissions, alongside its flexibility to regenerate with intermittent energy sources.

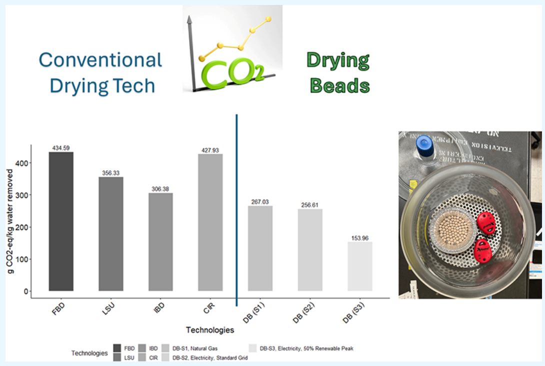

1. INTRODUCTION

Drying is crucial in preserving paddy rice's quality, shelf life, and milling efficiency, which sustains over half of the global population. Freshly harvested paddy has an initial moisture content on a wet basis (MC_{wb}) of 24% or more, making it susceptible to degradation.[1,2] Proper drying, which reduces the MC_{wb} to around 12−14% for safe storage, is essential to prevent the growth of microorganisms such as mold and bacteria and, subsequently, to mitigate spoilage, diminished quality, and substantial food losses.[3,4]

While conventional paddy drying methods, such as ambient air-drying or direct sun-drying, require minimal investment and are easy to implement, they are often inconsistent and weather-dependent, yielding suboptimal results and leading to significant food loss.[5,6] In contrast, mechanical drying methods like FBDs and spouted bed dryers offer improved drying performance in terms of speed, capacity, and quality.[7−9] However, these methods have high total energy consumption and rely on fossil fuels as an energy source, contributing to substantial greenhouse gas (GHG) emissions and high drying costs.[10,11]

Specifically, paddy rice drying accounts for around 55% of the total energy used in the production and processing stages.[12] Natural gas, the primary fuel for drying crops, produces high GHG emissions, and paddy rice drying contributes to 9−11% of the agricultural GHG emissions.[12,13] Efficient drying methods can preserve rice losses, including the HRY and cracking rate, thereby reducing the overall carbon footprint of paddy rice production. As the global community seeks to mitigate climate change, pursuing innovative paddy rice drying technologies has become increasingly important.

Desiccants have shown potential for moisture control across various industries.[14−16] Desiccants absorb moisture from the environment, lowering the relative humidity (RH) and, therefore, can accelerate the drying process.[17] However, their moisture absorption capacity is finite and declines over time, requiring desiccant regeneration. The total energy required for desiccant regeneration in the drying bead (DB) system is higher compared to the energy consumed during the crop drying phase, which underlines the need to consider the

Received: June 9, 2024
Revised: August 15, 2024
Accepted: August 20, 2024
Published: August 26, 2024

https://doi.org/10.1021/acsomega.4c04153
ACS Omega 2024, 9, 38142−38152

regeneration energy demand when comparing drying technologies.[18−21]

Zeolite-based DBs, a desiccant type, have gained increasing attention in crop drying.[22] However, a comprehensive understanding of the regeneration conditions, specifically in terms of temperature, time, and total energy consumption, still needs to be determined. One desiccant that has been beneficial in moisture control is the zeolite 13X molecular sieve, a sodium form of the crystal structure with a large pore size (10 Ångströms), which leads to a high adsorption capacity of 0.12−0.14 kg of water per kg of desiccant.[23] Al Ezzi et al. reported that 55% saturated zeolite 13X desiccant could be regenerated to 2.5% MC_{wb} in 15 min at 100 °C, while fully saturated desiccants require 65 min at 120 °C.[24] Nevertheless, there remains a gap in our understanding of optimal regeneration conditions for zeolite DBs.

This study builds on previous research that examined DB as a desiccant for paddy drying within a lab-scale vertical dryer known as the DB system. The DBs, developed by the Rhino Research Group in Bangkok, Thailand, are designed for mechanical stability and reusability.[19] The DB system dehydrates and heats the air flowing through a drying chamber, which is then used to reduce the paddy's MC_{wb}. Results showed that the quality of rice, measured by the head rice yield (HRY), total milling yield, and kernel color, met the commercial U.S. No. 1 grade standards and could offer faster drying times in comparison to convective drying at 50 °C, highlighting the potential efficacy of DBs in paddy drying applications.[25]

To evaluate the overall performance of the DB system and understand its regeneration properties, including the relationship between the temperature and drying time and the required total energy input, we employed the TA Instrument SDT Q600 Simultaneous TGA/DSC instrument (SDT Q600; TA Instrument, New Castle, DE, USA). This instrument, which combines differential scanning calorimetry (DSC) and thermogravimetric analysis (TGA), is essential for analyzing material behavior under thermal stress. Our approach is informed by studies like that of Barreneche et al.,[26] who utilized DSC and TGA to investigate the desorption process in materials such as $CaCl_2$ and zeolite. By logging the heat flow rate and weight changes during the DB regeneration process with an SDT Q600, we can quantify the total energy required to reduce the MC in the DB through time.

Once we quantify the total energy required to regenerate DBs, we can compare the paddy drying total energy consumption and GHG emissions of the DB system to those of conventional drying methods. For this study, we applied a scenario-based approach to evaluate the carbon emissions related to the DB system under three different paddy rice drying conditions. These scenarios consider the use of California's electrical grid during regular hours and renewable peak-generation hours, focusing on times when the grid's solar energy percentage is at its highest. This approach offers a better understanding of the environmental impact of the DB system applied to dry paddy rice.

This study focused on three objectives: first, to quantify the total energy needed to regenerate a single DB; second, to identify the optimal temperature and time required for a DB regeneration; and third, to compare the total energy requirements and associated carbon emissions of DB drying to those of conventional methods.

2. MATERIALS AND METHODS

The study was conducted in the Plant and Environmental Laboratory and the Postharvest Engineering Laboratory at the University of California, Davis (UC Davis), using a TA Instruments SDT Q600 instrument, as shown in Figure 1. The

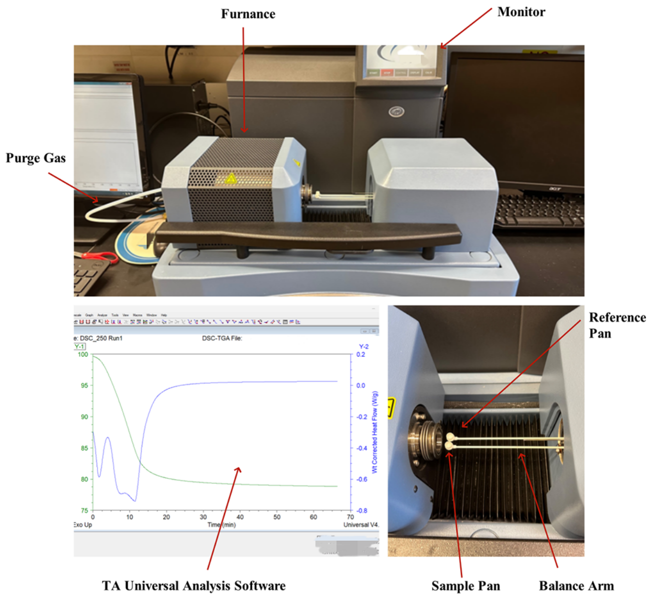

Figure 1. Photo of the SDT Q600 setup.

SDT Q600 contains (1) a furnace, which controls the environmental temperature to heat or cool samples; (2) a purge gas tube that injects 99.999% nitrogen to create an inert atmosphere to prevent oxidation and ensure uniform heat distribution within the furnace; (3) a sample pan, holding the DB or sample, while the reference pan is empty; (4) a balance arm that measures weight changes in the sample as it undergoes the thermal processes; and (5) a monitor and Universal Analysis software, which displays real-time graphical data and controls the instrument while continuously monitoring the sample's weight. Experiments conducted from December 2022 to March 2023 were designed to study DB regeneration on six temperature settings, categorized into three groups: low (90, 120, and 150 °C), medium (200 and 250 °C), and high (350 °C) temperatures. Three trials were randomly conducted for each temperature setting for 18 experimental runs.

This section outlines the detailed procedural steps taken during and after the experimental runs. These procedures are visualized through two flowcharts, as shown in Figure 2, which delineate the sequence of actions and data handling methodologies used. The first chart illustrates the experimental setup and execution, ensuring each phase is precisely controlled. The second chart details the subsequent data processing steps required for deriving clear insights from the experimental data.

The experimental procedures for our study are outlined in the flowchart provided. This chart begins with the preparation of the DB samples and includes detailed steps such as the calibration of the SDT Q600 instrument, placement of the DB samples, and initiation of the experiment under a controlled nitrogen gas atmosphere. Each step is carefully designed to ensure precision and reproducibility, as shown in the flowchart.

Following the completion of experimental runs, the postexperimental procedures, as illustrated in our flowchart,

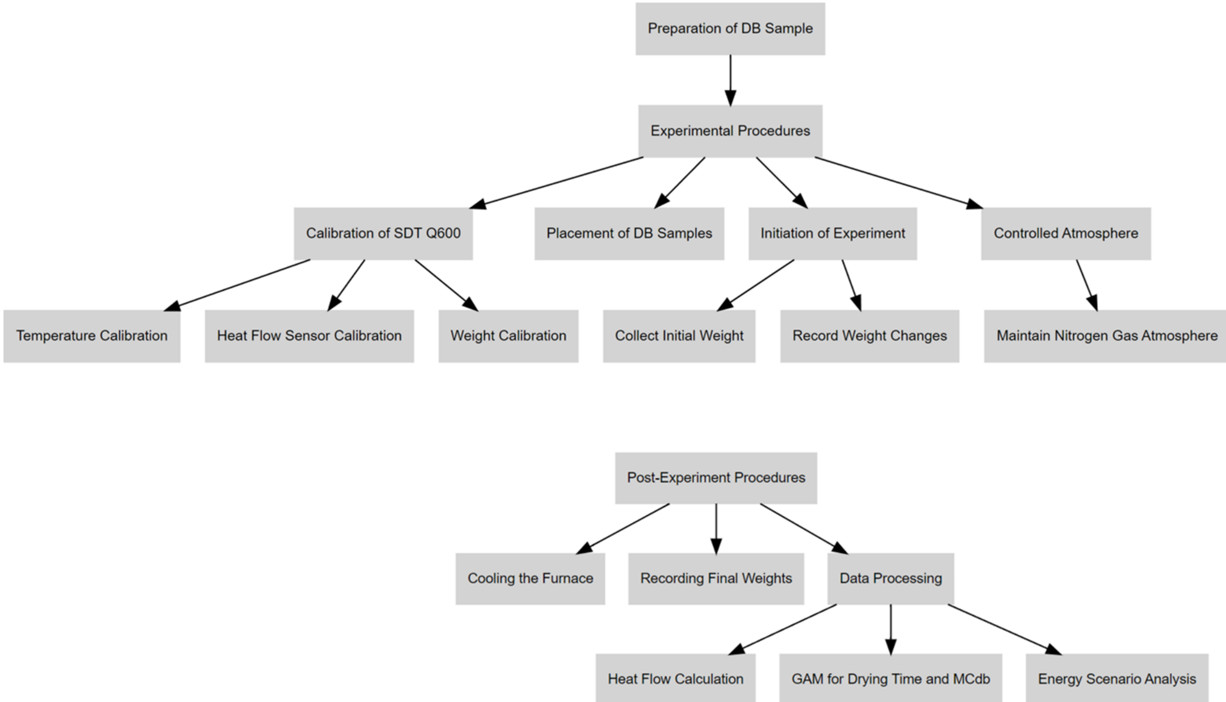

Figure 2. Flowchart of the experimental procedure.

involve cooling the furnace, recording the final weights of the samples, and processing the collected data. This includes calculations of heat flow, general additive modeling for drying time and moisture content database (MC_{db}), and energy scenario analysis, each critical for interpreting the results and ensuring the integrity of our findings.

2.1. Preparation of the DB Sample. Ensuring uniformity in the size and weight of the DBs was critical in achieving consistent experimental results. Considering the SDT Q600 has a maximum capacity of 200 mg and DBs' water retention of 30%, we set a maximum weight limit of 120 mg for each DB. The initial phase involved measuring the diameter of 20 DBs, each within the maximum weight limit, using a Fisherbrand Traceable Digital Caliper. This measurement established a reference diameter for the subsequent selection process, revealing that DBs up to 120 mg typically have a diameter not exceeding 6 mm. Using a Fritsch ANALYSETTE 3 SPARTAN vibratory sieve shaker, we expanded our sample set to include 90 DBs, all conforming to the maximum diameter and weight limits.

DBs were immediately stored in an airtight desiccator at approximately 25 °C to prevent moisture exchange while providing a consistently controlled environmental RH. To achieve this, 50 g of potassium chloride salt was placed at the bottom of the desiccator and mixed with 32.8 mL of distilled water to create a saturated solution, generating an environment with 80% RH.[27] This was intended to simulate conditions from a previous DB system experiment that evaluated the performance of drying paddy rice at 80% RH (Ying et al.,[25] Submitted). Two Kestrel Drop D3 wireless temperature, humidity, and pressure data loggers (Kestrel Instrument, Boothwyn, PA, USA) were placed inside the desiccator to continuously monitor the temperature and RH.

2.2. Experimental Procedures. The initial phase of our experiment involved a multistep calibration of the SDT Q600, crucial for accurate results. First, temperature calibration was performed to ensure the thermal readings were accurate, which involved cross-referencing the instrument's readings with known temperature standards, in the case of the filling point for zinc. Following this, we adjusted the heat flow rate sensor, a crucial component for measuring thermal energy transfer during the regeneration process. We ensured the precision of our measurement equipment through a rigorous calibration.

The SDT Q600 was chosen for its precise weight sensitivity of ±0.0001 mg and temperature accuracy of ±1 °C, essential for the accurate measurement of DB weights and thermal properties during the regeneration process. This instrument is specifically designed to maintain a highly controlled internal environment, which mitigates the impact of external environmental factors, such as fluctuations in laboratory temperature and humidity. The instrument's advanced thermal regulation system and inert gas atmosphere ensure that the experimental conditions are stable and consistent.

The enclosed design of the SDT Q600 plays a pivotal role in shielding the experiments from potential variability in air composition and ambient humidity. This level of environmental control is maintained throughout all experimental runs, as confirmed by the consistent results obtained for multiple trials. Regular calibration against recognized standards and the high degree of control provided by the instrument ensure that observed changes in DB weights and thermal properties accurately reflect true experimental outcomes, not influenced by external environmental variability.

Second, weight calibration was performed using a standard weight (20 mg) per the manufacturer's guidelines, ensuring that the temporal changes in the DB's weight during the experiment could be precisely measured. Third, the operational parameters for the experiment were configured using the Universal Analysis software using the "ramp" heating mode, wherein the temperature was programmed to increase at a controlled rate of 20 °C/min to the predetermined target

https://doi.org/10.1021/acsomega.4c04153
ACS Omega 2024, 9, 38142−38152

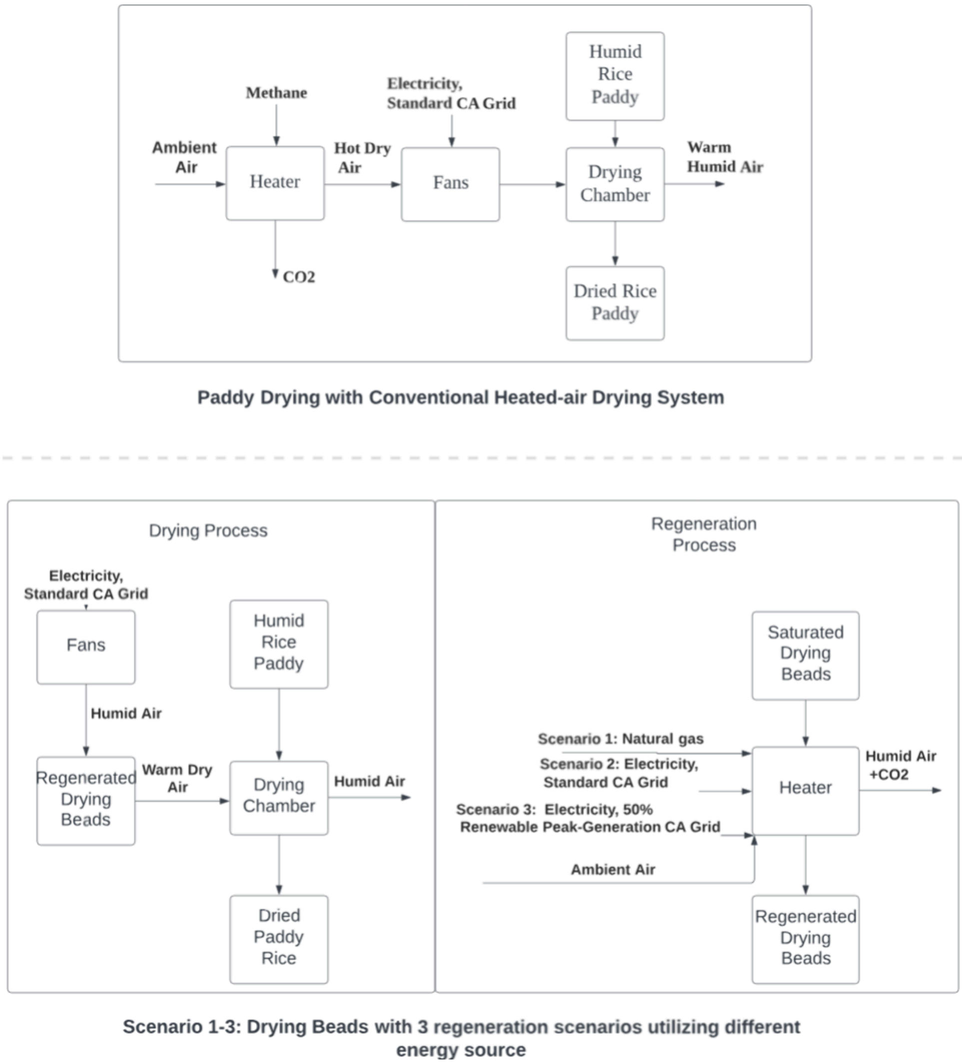

Figure 3. Flowchart depicting four paddy drying scenarios with DBs and conventional heated air dryers.

temperature. This target temperature was maintained for 60 min for each experiment.

Before the experiment, the sample pan was thoroughly cleaned with a microtorch for 15 s. When the experiment was initiated, DB samples were placed into the sample pan, and care was taken to carefully and quickly reopen the furnace to prevent DB samples from moisture loss. The initial weight of the DBs was collected and recorded every 0.5 s. Throughout the experiment, the STD Q600 system was flushed with nitrogen gas at a purity level of 99.999% and a 100 mL/min flow rate to ensure a controlled experimental atmosphere. The experiment was concluded when the weight of the DB sample changed by less than 0.005 mg in 5 min.

To determine the dry weight of the DBs, we assume that the DBs are thoroughly dried, as per the manufacturer's indication that they can be completely dehydrated above 400 °F (204 °C). Given that our experimental temperatures of 250 and 350 °C exceed this threshold, we consider these conditions sufficient to achieve complete dehydration. Therefore, the final weight of the DB samples, which exhibited minimal change (less than 0.005 mg over 5 min), is considered the dry weight. This assumption is substantiated by the fact that the smallest weight change measured represents less than 1/20,000th of the total DB weight (typically between 120 and 200 mg), confirming that the DBs reached a stable and effectively dry state. We used this final weight as the dry weight for all subsequent calculations and analyses.

2.3. Postexperiment Procedures. After the experiment concluded, the cooling fan was activated, the nitrogen supply was automatically turned off, and the compressed air gas valve was opened to allow compressed air to flow through the furnace to initiate the cooling process. Since our experiment was initiated at 25 °C, it was crucial to cool the furnace to 23 °C or lower before starting subsequent experiments.

2.4. Data Processing. Drying temperature, heat flow rate over time, and sample weight were logged into a .CSV format file from TA Universal Analysis software. To calculate the total overall required energy, we calculated the area under the heat flow rate curve over time by applying the Trapezoidal Rule, as detailed in various research.[28,29] During the DB regeneration phase, heat transfer is calculated based on the assumption of standard electric resistance heating. According to Dincer,[30] an electrical resistance heater can achieve 100% efficiency by converting all electrical energy into heat. Therefore, the total energy values reported in this study reflect the minimum total energy necessary to regenerate DBs under controlled, saturated conditions by using laboratory-scale fans. These findings are relevant to high-efficiency laboratory environments.

https://doi.org/10.1021/acsomega.4c04153
ACS Omega 2024, 9, 38142−38152

We conducted a two-sample t test using R to compare the total corrected required total energy and drying time between different experimental runs. We analyzed the drying time of DB at different temperatures and created bar graphs with error bars to show the mean and standard deviation. We also used the STD Q600 system balance to measure weight changes and calculate the MC_{db} changes for each experiment. We plotted these data against drying time to understand how the MC_{db} changes. To analyze this data more accurately, we used a generalized additive model (GAM). GAM is applied to model complex, nonlinear relationships in time-series data and helps us understand the intricate variations in MC_{db} over time. The GAM fits the MC_{db} data over time with a smooth function, providing a detailed view of the dynamics of the drying process. The model's goodness-of-fit was verified through R-squared values and corresponding residuals.[31]

2.5. Energy Scenario Analysis. The upper portion of Figure 3 shows the conventional heated-air-drying scenario within California's energy landscape, where we assumed that natural gas-fueled heaters account for 80% of the total energy use and the remaining 20% is attributed to grid electricity to power fans and other auxiliary systems.

This study also explored three scenarios for DB technology, each characterized by its unique emission factors influenced by the timing of electricity consumption. The first scenario utilizes a standard natural gas heater to regenerate the DB, while electricity from a standard CA Grid powers the fans and control systems. The second scenario employs standard grid electricity for all DB-related activities, thereby altering the resulting emission factor. The third scenario specifically allocates 50% renewable peak-generation electricity and 50% standard grid electricity for the regeneration process.

Additional data from the California Air Resource Board indicated that the average emission factor for California's electrical grid was 0.19 metric tons CO_2-eq/MWh, or 0.0528 CO_2-eq/MJ.[32] This metric did not include the inefficiencies caused by line losses during electrical transmission and distribution, and according to data from the Monthly Renewable Performance Report spanning July 2022 to June 2023, wind and solar energies alone provided 103.5−106.8% of California's peak-hour load requirements.[33] This suggests that if we solely use renewable energy, then the carbon intensity of electricity in peak hours could even be negative. Therefore, the third scenario, which involves using 50% renewable peak-generation electricity for regeneration, has an estimated emission factor of 0.0264 kg of CO_2-eq/MJ. This is roughly half of the average emissions for California's grid.

2.6. MC_{db} and Loss and GHG Emission Calculations. The assessment of the water gain rate for DBs relative to the water loss from paddy was previously made using a laboratory-scale vertical dryer. Prior to the experiment, the initial weights of the regenerated DB and dried paddy were measured. In the experimental setup, the DBs were accommodated in the desiccant chamber, while the paddy was positioned in the sample chamber. Weight variations in both the desiccant and sample chambers were monitored using load cells (SMT1-56/112, Interface, Arizona, USA). A data acquisition unit (NI 9265, 16-bit, 0−20 mA, cDAQ-9178 Compact Chassis, National Instruments, Austin, TX, USA) interfaced with the vertical dryer. In alliance with LabVIEW 2018 (National Instruments, Austin, TX, USA), this setup facilitated real-time monitoring and data recording. To maintain consistency, all experimental procedures were executed in an indoor environment, with the room temperature rigorously held at 25 °C.

The experiment concluded with recording of the final weights of the DBs and the paddy. The weight the DB gained and the corresponding weight loss of paddy were utilized to compute the DB's water gain/loss ratio. This calculation was used to assess the efficiency of the DB in extracting moisture from the paddy during the drying process. According to this study, the DB's water gain/loss ratios were found to be 86% ± 1.8%, 95% ± 2.1%, and 105% ± 1.9% during three different experimental runs. Differences in the DB's water gain/loss ratios can be primarily attributed to the varying drying times resulting from the differing initial moisture contents in the paddy rice samples. This variation was noted even though the inlet air temperature, humidity, and speed were maintained at constant levels.

The MC of DB was assessed based on two assumptions. First, the DB was completely saturated within an 80% RH environment. Second, the TGA experiment regenerated the DB to 0% MC_{db}, where the weight recorded at the end of the experiment was the weight of the dried DB. The difference between the initial and final weights of the DB during the experiment indicated the weight of the evaporated water. The MC of the DB was expressed on a dried basis (MC_{db}), and it was calculated as follows:

$$MC_{db} = \frac{\text{Weight of evaporated water}}{\text{Weight of dried DB}} \tag{1}$$

Equation 2 was used to calculate the GHG emissions to remove 1 kg of water from paddy associated with different conventional drying technologies while assuming that natural gas is the primary fuel source used in the industry at a heat transfer rate of 81%, as reported by Amantea.

$$\text{GHG} = \frac{H_a \times E_i}{H_t} \times \text{Ef}_n + P_e \times E_i \times \text{Ef}_e \tag{2}$$

where H_a is the energy in a paddy rice drying system used to heat the air to dry the paddy rice, which equals 80%; P_e is the energy in a paddy rice drying system used to power the fans and control systems, which equals 20%; E_i is the total energy used by a drying system to evaporate 1 kg of water from paddy (MJ/kg); H_t is the heat transfer rate of the natural gas, which is 81%; Ef_n is the energy used to power electrical components in paddy rice drying systems, including fans, control system, motors, and sensors, which equals 20%; and Ef_e is the California electricity emission factor, 0.0528 kg $CO_{2\text{-eq}}$/MJ for average and 0.0264 kg $CO_{2\text{-eq}}$/MJ for 50% renewable peak-generation hours (CARB, 2020).

In the case of the DB drying systems, which use a bed of DBs to dehydrate and heat the air, we assumed that the electrical components accounted for 20% of the total energy usage. In comparison, the DB regeneration process accounted for the remaining 80%. Based on this, the GHG gas emission attributed to the use of DBs per kilogram of paddy dried (GHG_d) for a desiccant-based dryer, expressed in kilograms of CO_2-equivalent per kilogram of water removed from the paddy (kg of CO_2-eq/kg of water), was calculated as in eq 3.

$$\text{GHG}_d = (E_r + E_o) \times \text{Ef}_e \tag{3}$$

where E_r is the specific energy consumption for the regeneration process (MJ/kg water removal) and E_o is the

https://doi.org/10.1021/acsomega.4c04153
ACS Omega 2024, 9, 38142−38152

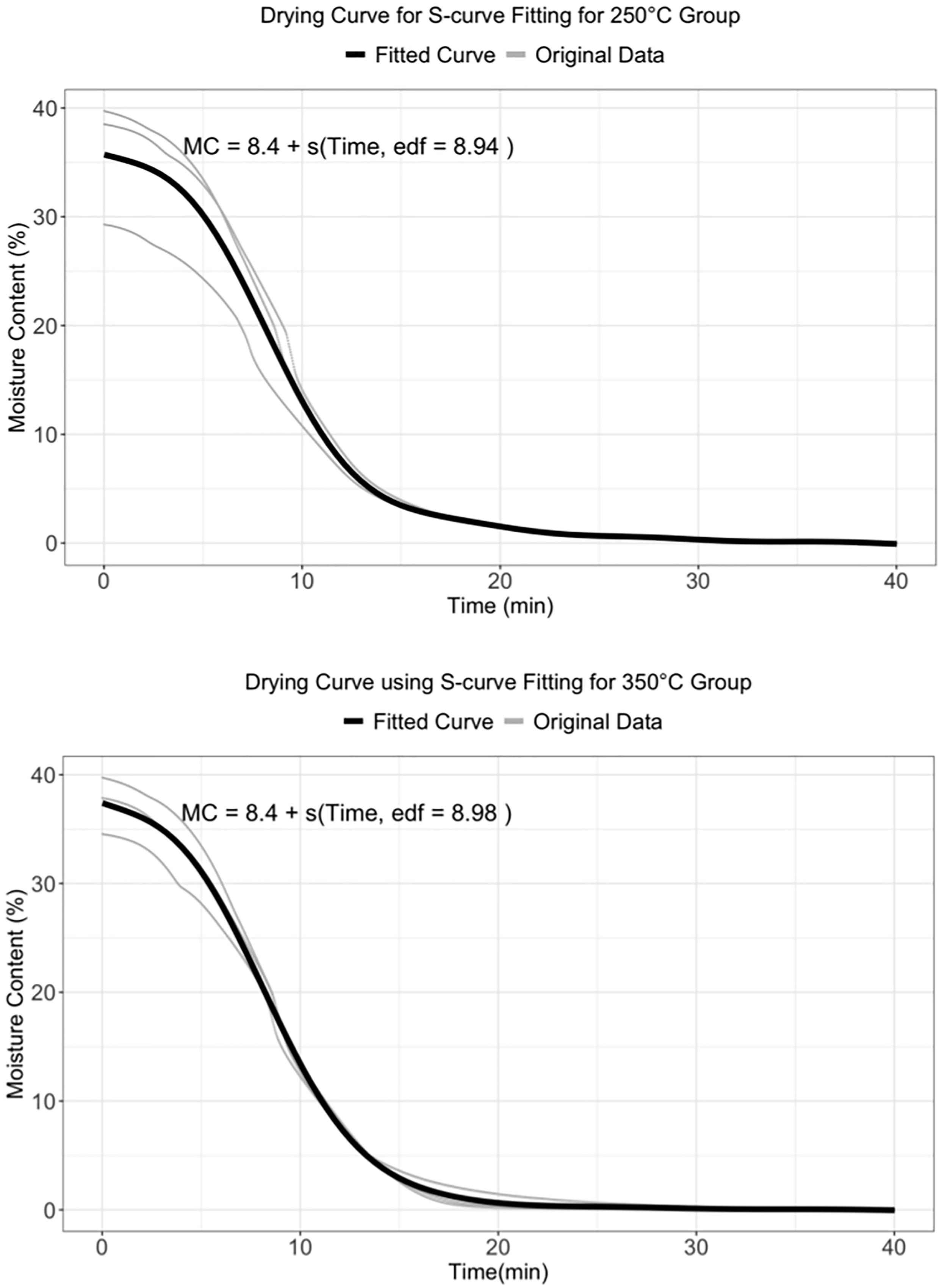

Figure 4. Drying curves for DB regeneration for 250 °C (a) and 350 °C (b) TGA tests.

specific energy consumption for the operational process (MJ/kg water removal).

https://doi.org/10.1021/acsomega.4c04153
ACS Omega 2024, 9, 38142−38152

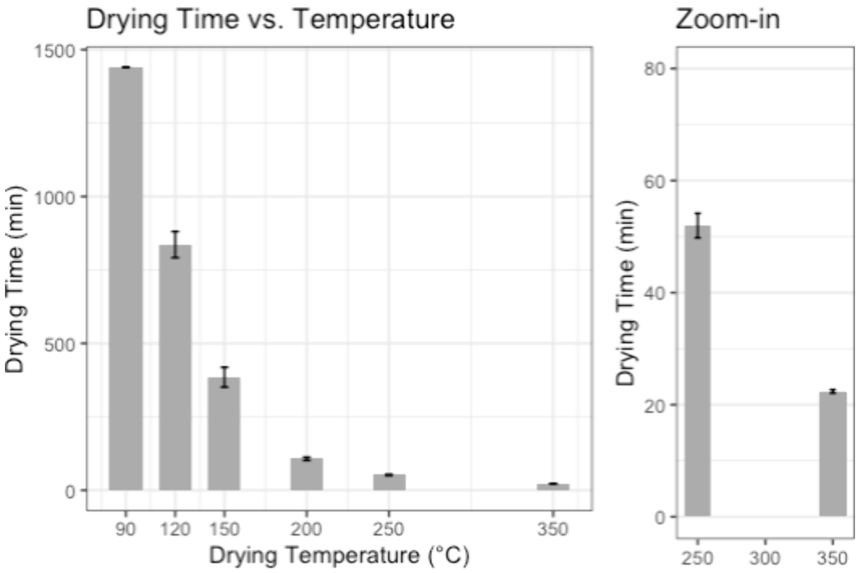

Figure 5. Drying time vs temperature for the 250−350 °C range.

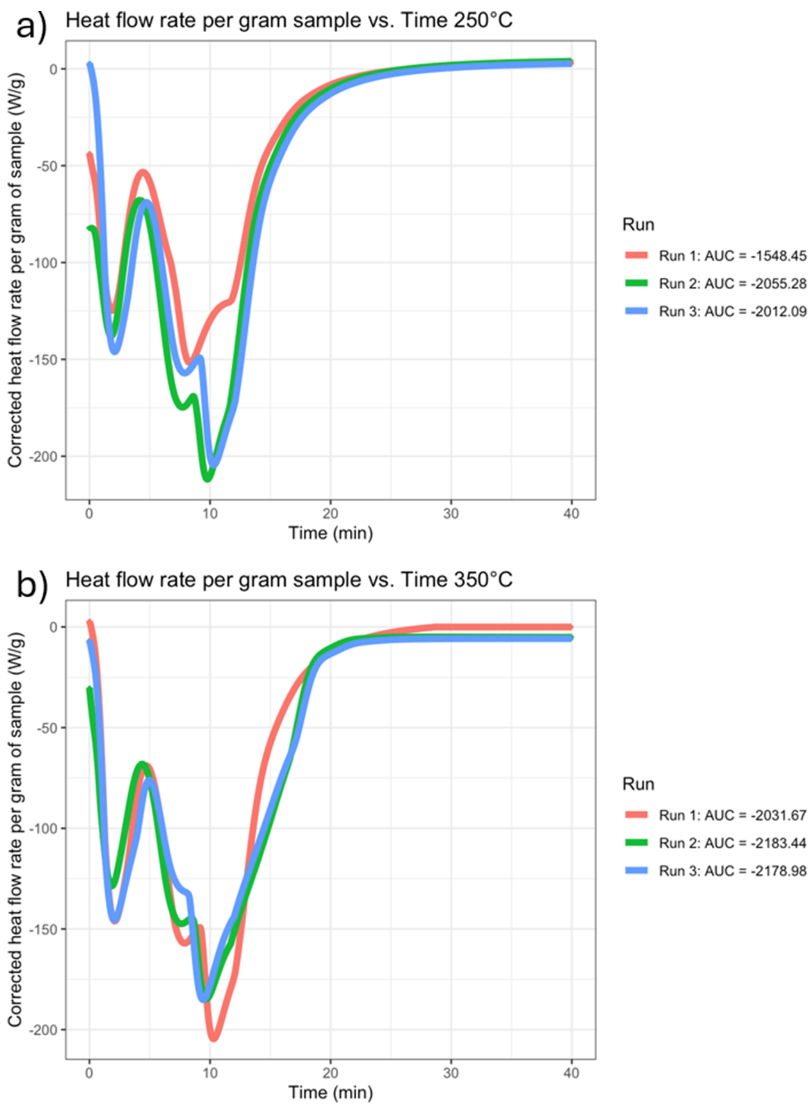

Figure 6. Total corrected heat flow rate per kilogram of DB (kW/kg DB) at 250 °C (a) and 350 °C (b).

https://doi.org/10.1021/acsomega.4c04153
ACS Omega 2024, 9, 38142−38152

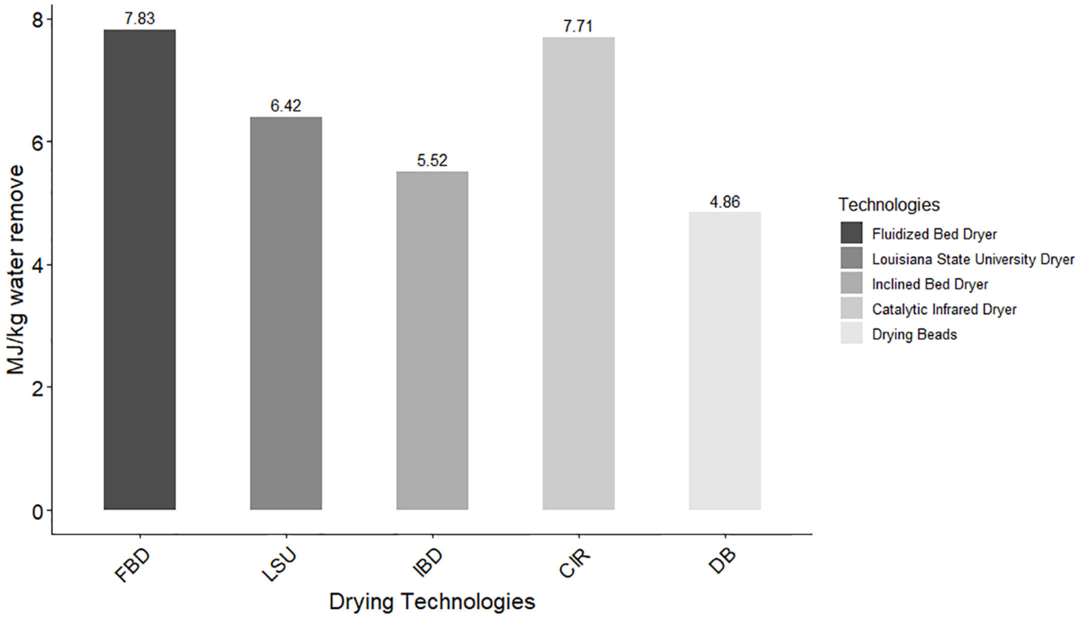

Figure 7. Energy consumption of paddy drying for different drying technologies.

3. RESULTS AND DISCUSSION

Figure 4 presents the DB regeneration (drying) curves for the 250 and 350 °C temperature groups. Even though the transitions between the phases are not sharply demarcated, the shape of the DB regeneration curves generally follows the trend of a conventional three-phase drying curve observed in multiple research studies.[34,35,36] Initially, there is a period where the rate of regeneration rapidly increases, which corresponds to Phase I, where the DB and internal water likely warm up. As the regeneration process continues, the curve shows a region where the DB regeneration rate appears relatively stable, similar to the constant rate period known as Phase II, where the water content in the DB decreases rapidly. Toward the end of the curve, a gradual reduction in the drying rate is observed, which could indicate the falling rate period or Phase III, where the moisture removal is relatively constant. However, due to the absence of clear phase transitions in the data, this interpretation is more suggestive than definitive, and the DB regeneration curves should be regarded as indicative of an overall regeneration trend rather than a precise phase-by-phase breakdown.

Upon closer examination of the 250 °C group, one of the DBs exhibited a lower water-holding capacity compared with the other two beads in the 250 °C group and all three beads in the 350 °C group. This variation is potentially due to individual differences in water capacity among the DBs. Specifically, the water-holding capacity ranged from 30 to 42.3% of the dry weight. These values exceed the manufacturers' specifications, which claimed a maximum water-holding capacity of 20–25% of the dry weight and previous oven incubation tests that showed a DB water-holding capacity ranging between 28 and 30%.[25] The higher sensitivity, accuracy, and precision of the standalone TGA technique applied in this study contributed to the discovery of an increased DB moisture-holding capacity compared to previous studies. Notably, four out of the six DBs tested exhibited moisture-holding capacities above 38%, with one DB around 30%, reflecting the variability among the individual beads.

Figure 5 shows the average time it takes to regenerate a DB, with error bars indicating the standard deviation. These times were recorded at six different temperatures, ranging from 90 to 350 °C. The results showed that the average regeneration time varied between 1440 and 16 min. Higher temperatures led to a shorter regeneration time due to reduced MC_{db}, while regeneration at 90 °C was not successful, as the DB final MC_{db} ranged between 86 and 88%.

DBs were fully regenerated at 120, 150, 200, 250, and 350 °C within 813 ± 66.2, 350 ± 35.1, 160 ± 13.7, 52 ± 2.2, and 22 ± 0.31 min, respectively. Temperatures exceeding 350 °C were not evaluated due to safety and practical implications associated with achieving such elevated temperatures in an agricultural context.

Figure 6 illustrates the heat flow rate results during the regeneration process of the DB, highlighting two distinct phases characterized by pronounced peaks. The first peak occurs within the initial 2 min of the experiment, marking the rapid warming of the DB. This peak declines by the 4 min mark as the system temperature stabilizes at 100 °C for both the 250 and 350 °C regeneration temperatures. The decrease in the heat flow at this stage primarily results from the consumption of latent heat, which facilitates the evaporation of surface moisture and the migration of internal water from the core to the surface of the DBs.

This initial peak is critical for understanding the thermal responsiveness of the DBs to the applied heat, indicating a rapid surface moisture removal, which is crucial for the efficiency of the regeneration process. The presence of this peak, especially its decline at lower regeneration temperatures, provides valuable insights into the thermal dynamics of moisture evaporation within the DB system.

Contrary to the single peak observed by Barreneche et al. in dehydrating zeolite materials,[26] our experiments display a second, significant peak. This peak likely signifies the deeper internal desorption process within the DB core, as supported by the lower peak intensities in subsequent experimental runs with a reduced moisture content in the DBs (MC_{db}). These observations suggest a dynamic variance in the moisture

https://doi.org/10.1021/acsomega.4c04153
ACS Omega 2024, 9, 38142–38152

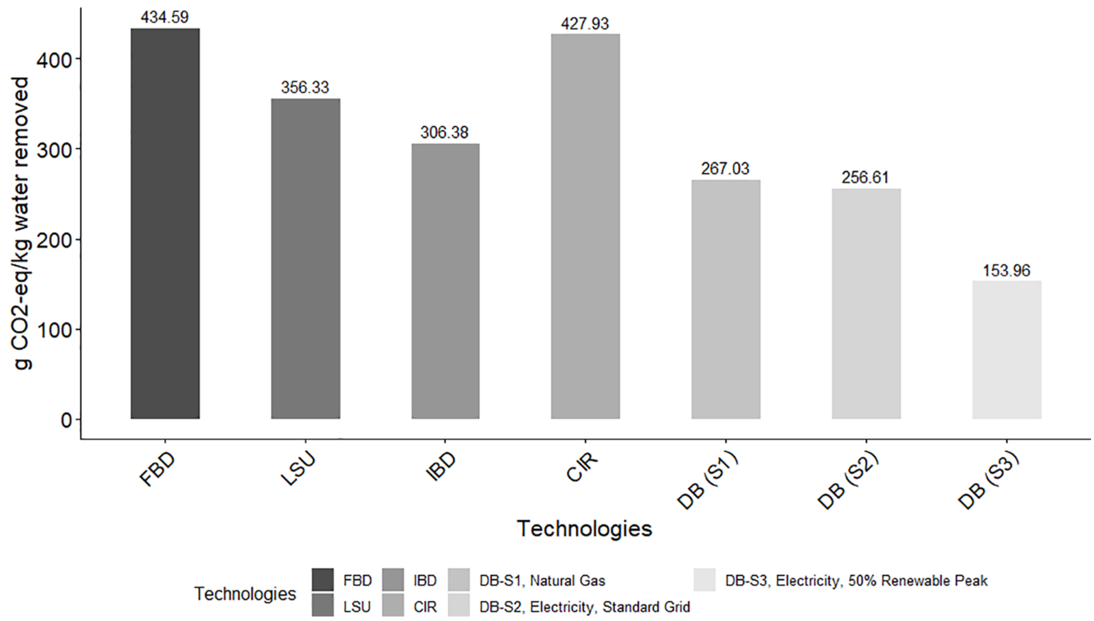

Figure 8. Carbon emission intensity for different conventional heat-air-drying technologies and DB scenarios.

absorption and desorption processes, which are critical for optimizing the DB's performance in practical applications.

Post regeneration, a stabilization in heat flow is observed, indicating the minimum energy required to maintain the DBs at operational temperature. Analyzing the area under the curves in Figure 5 not only quantifies the total energy involved in the regeneration process but also offers a comprehensive understanding of the DB's thermal behavior when fully saturated. Such an analysis is essential for assessing the energy efficiency of the regeneration process and its environmental impact.

For regeneration temperatures of 250 and 350 °C, the total energy required to completely regenerate a bead is quantified at 2032 and 2136 kJ per kg of dried DB, respectively. The small difference in the heat flow between these temperatures highlights the efficiency of the insulation and temperature control within the DSC/TGA instruments. Additionally, the similar corrected heat flow rates at both peaks for the two temperature settings, measured at 150 and 200 kW/kg of DB, underscore that a higher temperature does not necessarily equate to a proportional increase in energy consumption. This observation points to the possibility of more efficient heat transfer mechanisms, such as enhanced radiation or convection, being more effective at higher temperatures. This enhanced analysis directly addresses the intricacies of heat transfer within the DB system and provides a deeper understanding of the implications for energy use and efficiency in agricultural drying technologies.

According to this study, the average MC_{db} of DB was found to be 41%. This suggests that 1 kg of dried DB could extract at least 0.41 kg of water before becoming saturated. It was estimated that for every 1 kg of water lost from the paddy rice, the DB gained 0.95 kg of weight and lost 0.05 kg through evaporation. Based on the ratio of paddy water loss to DB weight gain, and if 1 kg of dried DB can absorb 0.41 kg of water from the air, it can be estimated that a minimum of 2.32 kg of DB would be needed to extract 1 kg of water from paddy under this configuration. Therefore, it can be estimated that 4859 kJ of energy is used to evaporate 1 kg of water, with an average heat flow of 2095 kJ/kg between 250 and 350 °C.

Figure 7 provides a comparative analysis of the calculated energy consumption of the DB system in relation to other commercially available drying technologies, such as fluidized bed dryers (FBDs), catalytic infrared drying, Louisiana State University dryers, and inclined bed dryers. For the DB system, our approach involves extrapolating the total energy requirements from the measured heat energy by factoring in an additional percentage to account for operational energy, which primarily includes the usage of fans and control systems. Based on insights from this study combined with previous research, the DB system requires less energy in comparison to other drying technologies.[37] Our approach intentionally errs on the side of overestimation to ensure a comprehensive assessment of energy needs, considering the worst-case scenario. Previous studies have reported that the additional operational energy over the base heat energy is relatively low in rice drying, constituting about 4−5% of the total consumed energy.[38]

Figure 8 shows the comparison between GHG emissions for DB systems and conventional heated-air-drying methods in removing 1 kg of water. The DB system yielded less GHG emissions in the three energy scenarios, ranging from 153.96 to 267.03 g of CO_2-eq/MJ, lower than the average emissions of 378.81 g of CO_2-eq/MJ for conventional drying techniques. Further dissection of the scenarios reveals distinct insights. Scenario 2, which utilized electricity from the Standard California Grid, showed a slight advantage in terms of lower emissions compared with Scenario 1. More importantly, Scenario 3 demonstrated significant potential for reducing GHG emissions by integrating 50% renewable electricity during peak hours in the DB regeneration process. This scenario highlights the impactful role of renewable energy sources in enhancing the environmental performance of drying technologies.

In the California energy landscape, the year-to-date average for renewable energy generation stood at 37.96%,[33] surpassing the national average of 21.5%.[39] The utilization of renewable energy sources like wind and solar for DB system regeneration

https://doi.org/10.1021/acsomega.4c04153
ACS Omega 2024, 9, 38142−38152

offers a considerable opportunity to reduce the carbon footprint and environmental impact. It is important to note that these results are specific to the California grid environment, known for its low carbon intensity, making our findings particularly relevant to this region. The varying energy generation profiles must be considered when implementing similar technologies in different regions.

California's commitment to renewable energy is on an upward trajectory. As per the 2021 SB 100 Joint Agency Report, the state's renewable electricity production, currently at about 35,000 MW, is projected to increase to 73,000 MW by 2030 and to 183,000 MW by 2045, with the ultimate goal of achieving 100% clean electricity.[40] This shift toward renewable energy is set to substantially reduce carbon emissions from electricity use, including in industrial processes like drying.

In contrast to DB-utilizing systems, conventional drying technologies rely on natural gas. Although they could benefit from California's cleaner grid, transitioning to renewable energy sources may take considerable time. Unlike conventional dryers, which typically operate continuously, DB systems can utilize off-peak electricity and that from intermittent renewables. This advantage is particularly pronounced in California, but the principle holds potential for other regions as they progress toward cleaner energy solutions.

4. CONCLUSIONS

This study explores the thermal behavior and moisture absorption characteristics of the DB regeneration process as applied to paddy drying within a controlled laboratory environment and the potential to leverage renewable electricity to reduce carbon emissions in the drying process. Our analysis identified two distinct thermal phases, each marked by dual peaks in the heat flow data. These findings highlight specific temperature ranges as critical for optimizing the DB regeneration process, with energy consumption remaining consistent across these ranges thanks largely to the precise temperature control and isothermal conditions afforded by the SDT Q600 instrument.

Our results demonstrate that DBs exhibit a robust water-holding capacity, significantly enhancing their utility for paddy rice drying by potentially reducing the volume of DBs required. Comparative scenario analysis positions DB technology as a less-energy-intensive alternative to traditional drying methods, additionally offering the advantage of reduced GHG emissions when integrated with renewable energy sources, especially within the context of California's cleaner energy grid.

Future research should expand beyond the laboratory setting to evaluate the scalability and operational efficiency of DB technology in commercial agricultural settings. It is imperative to test the technology under varied geographic and climatic conditions to determine its efficacy and environmental impact at a scale. A comprehensive assessment of the full lifecycle of DB technology is essential to fully understand its overall environmental footprint.

The influence of energy sources and geographic factors on GHG emissions underscores the need for further investigation. Research aimed at synchronizing DB regeneration with the availability of renewable energy could markedly decrease the carbon emissions associated with drying paddy, potentially revolutionizing the environmental sustainability of paddy drying processes.

Additionally, operational challenges noted in this study, such as moisture loss during the transition of DBs to the oven for regeneration, warrant detailed examination in larger-scale implementations. Addressing these challenges is crucial to determine whether DB technology can be a viable and environmentally superior alternative to existing technologies in the paddy drying industry. Future studies should also explore the practical implications of DB usage within different energy grid contexts, particularly those dominated by nonrenewable sources, to provide a holistic assessment of its global applicability and sustainability.

■ AUTHOR INFORMATION

Corresponding Authors

Irwin R. Donis-González — *Department of Biological and Agricultural Engineering, University of California-Davis, Davis 95616-5270, United States*; Phone: (530) 752-8986; Email: irdonisgon@ucdavis.edu

Edward S. Spang — *Energy and Efficiency Institute and Department of Food Science and Technology, University of California-Davis, Davis 95616-5270, United States*; orcid.org/0000-0001-9883-078X; Phone: (530)-754-5447; Email: esspang@ucdavis.edu

Authors

Tianyu Ying — *Energy and Efficiency Institute, University of California-Davis, Davis 95616-5270, United States*; orcid.org/0000-0002-1848-204X

Alice Dien — *Department of Biological and Agricultural Engineering, University of California-Davis, Davis 95616-5270, United States*

Kurt Kornbluth — *Energy and Efficiency Institute and Department of Biological and Agricultural Engineering, University of California-Davis, Davis 95616-5270, United States*

Christopher W Simmons — *Energy and Efficiency Institute and Department of Food Science and Technology, University of California-Davis, Davis 95616-5270, United States*

Complete contact information is available at: https://pubs.acs.org/10.1021/acsomega.4c04153

Author Contributions

This paper has two corresponding authors who focus on distinct aspects of the research. Dr. Donis-González oversees the regeneration and DSC/TGA analysis, while Dr. Spang oversees the energy consumption and carbon emission components. The manuscript was written through contributions of all authors. All authors have given approval to the final version of the manuscript.

Notes

The authors declare no competing financial interest.

■ ACKNOWLEDGMENTS

This research project was sponsored by the Foundation for Food & Agriculture Research and the UC Davis Innovation Institute for Food Health. The authors would like to thank Dr. Bryan M. Jenkins for his support throughout the experiment.

■ NOMENCLATURE

DB	drying bead
DSC	differential scanning calorimetry
SDT Q600	SDT Q600 simultaneous TGA/DSC
TGA	thermogravimetric analysis

REFERENCES

(1) Gustavsson, J., Cederberg, C., Sonesson, U., Van Otterdijk, R., Meybeck, A. Global food losses and food waste. In *Save Food Congress*; Düsseldorf, Germany, 2021.

(2) Parfitt, J.; Barthel, M.; Macnaughton, S. Food waste within food supply chains: quantification and potential for change to 2050. *Philos. Trans. R. Soc., B* **2010**, *365* (1554), 3065−3081.

(3) Rahman, M. S.; Perera, C. O. Drying and food preservation. In *Handbook of Food Preservation*; Marcel Dekker: 1999; pp 173−216.

(4) FAO. *The State of Food and Agriculture 2019: Moving forward on food loss and waste reduction*. Rome. http://www.fao.org/3/ca6030en/ca6030en.pdf (accessed 2023-03-20).

(5) Imoudu, P. B.; Olufayo, A. A. The effect of sun-drying on milling yield and quality of rice. *Bioresour. Technol.* **2000**, *74* (3), 267−269.

(6) Zhang, N.; Wu, W.; Li, S.; Wang, Y.; Ma, Y.; Meng, X.; Zhang, Y. Comprehensive Evaluation of Paddy Quality by Different Drying Methods, Based on Gray Relational Analysis. *Agriculture* **2022**, *12* (11), 1857.

(7) Jittanit, W.; Srzednicki, G.; Driscoll, R. H. Comparison between Fluidized Bed and Spouted Bed Drying for Seeds. *Drying Technol.* **2013**, *31* (1), 52−56.

(8) Madhiyanon, T.; Soponronnarit, S. High Temperature Spouted Bed Paddy Drying with Varied Downcomer Air Flows and Moisture Contents: Effects on Drying Kinetics, Critical Moisture Content, and Milling Quality. *Drying Technol.* **2005**, *23* (3), 473−495.

(9) Tirawanichakul, S.; Prachayawarakorn, S.; Varanyanond, W.; Tungtrakul, P.; Soponronnarit, S. Effect of Fluidized Bed Drying Temperature on Various Quality Attributes of Paddy. *Drying Technol.* **2004**, *22* (7), 1731−1754.

(10) Golmohammadi, M.; Assar, M.; Rajabi-Hamaneh, M.; Hashemi, S. J. Energy Efficiency Investigation of Intermittent Rice Dryer: Modeling and Experimental Study. *Food Bioprod. Process.* **2015**, *94*, 275−283.

(11) Sarker, M. S. H.; Ibrahim, M. N.; Aziz, N. A.; Punan, M. S. Overall Energy Requisite and Quality Feature of Industrial Paddy Drying. *Drying Technol.* **2015**, *33* (11), 1360−1368.

(12) Kasmaprapruet, S.; Paengjuntuek, W.; Saikhwan, P.; Phungrassami, H. Life Cycle Assessment of Milled Rice Production: Case Study in Thailand. *Eur. J. Sci. Res.* **2009**, *30* (2), 195−203.

(13) Smith, P.; Bustamante, M.; Ahammad, H.; Clark, H.; Dong, H.; Elsiddig, E. A.; Bolwig, S. Agriculture, Forestry and Other Land Use (AFOLU). In *Climate Change 2014: Mitigation of Climate Change. Contribution of Working Group III to the Fifth Assessment Report of the Intergovernmental Panel on Climate Change*; Cambridge University Press: Cambridge, U.K., 2014; pp 811−922.

(14) Barati, A.; Kokabi, M.; Famili, M. H. N. Drying of Gelcast Ceramic Parts via the Liquid Desiccant Method. *J. Eur. Ceram. Soc.* **2003**, *23* (13), 2265−2272.

(15) Daou, K.; Wang, R. Z.; Xia, Z. Z. Desiccant Cooling Air Conditioning: A Review. *Renewable Sustainable Energy Rev.* **2006**, *10* (2), 55−77.

(16) Shanmugam, V.; Natarajan, E. Experimental Investigation of Forced Convection and Desiccant Integrated Solar Dryer. *Renewable Energy* **2006**, *31* (8), 1239−1251.

(17) Misha, S.; Mat, S.; Ruslan, M. H.; Sopian, K. Review of Solid/Liquid Desiccant in the Drying Applications and Its Regeneration Methods. *Renewable Sustainable Energy Rev.* **2012**, *16* (7), 4686−4707.

(18) Dien, A.; Momin, M. A.; Ying, T.; Spang, E. S.; Kornbluth, K.; Donis-González, I. R. Performance Evaluation of a Commercially Available Desiccant-Based Seed Drying System. *J. ASABE* **2022**, *65* (3), 633−643.

(19) Hay, F. R.; Thavong, P.; Taridno, P.; Timple, S. Evaluation of Zeolite Seed 'Drying Beads' for Drying Rice Seeds to Low Moisture Content Prior to Long-Term Storage. *Seed Sci. Technol.* **2012**, *40* (3), 374−395.

(20) Oladosu, T. L.; Baheta, A. T.; Oumer, A. N. Desiccant Solutions, Membrane Technologies, and Regeneration Techniques in Liquid Desiccant Air Conditioning System. *Int. J. Energy Res.* **2021**, *45* (6), 8420−8447.

(21) Shukla, D. L.; Modi, K. V. A Technical Review on Regeneration of Liquid Desiccant Using Solar Energy. *Renewable Sustainable Energy Rev.* **2017**, *78*, 517−529.

(22) Bradford, K. J.; Dahal, P.; Van Asbrouck, J.; Kunusoth, K.; Bello, P.; Thompson, J.; Wu, F. The Dry Chain: Reducing Postharvest Losses and Improving Food Safety in Humid Climates. In *Food Industry Wastes*; Academic Press: Cambridge, U.K., 2020; pp 375−389.

(23) Cherbanski, R.; Komorowska-Durka, M.; Stefanidis, G. D.; Stankiewicz, A. I. Microwave Swing Regeneration vs Temperature Swing Regeneration: Comparison of Desorption Kinetics. *Ind. Eng. Chem. Res.* **2011**, *50* (14), 8632−8644.

(24) Al Ezzi, A.; Ismael, L.; Fayad, M. A.; Jaber, A. A.; Al Jubori, A. M.; Al-Jadir, T.; Yusaf, T. Experimental Investigation of Dehumidification and Regeneration of Zeolite Coated Energy Exchanger. *Int. J. Thermofluids* **2022**, *15*, No. 100164.

(25) Ying, T.; Dien, A.; Kornbluth, K.; Spang, E.; Donis-González, I. Drying Performance and Quality Preservation of Calrose Rice Paddy Using Convective Zeolite-Based Desiccant Drying. *J. ASABE* **2024**, submitted for publication.

(26) Barreneche, C.; Fernández, A. I.; Cabeza, L. F.; Cuypers, R. Thermophysical Characterization of Sorption TCM. *Energy Procedia* **2014**, *48*, 273−279.

(27) O'Brien, F. E. M. The Control of Humidity by Saturated Salt Solutions. *J. Sci. Instrum.* **1948**, *25* (3), 73.

(28) Abramowitz, M.; Stegun, I. A., Eds. *Handbook of Mathematical Functions with Formulas, Graphs, and Mathematical Tables*; U.S. Government Printing Office: 1968.

(29) Whittaker, E. T.; Robinson, G. *The Calculus of Observations: A Treatise on Numerical Mathematics*; Blackie and Son Limited: 1928.

(30) Dincer, I. Energy and Exergy Efficiencies. In *Comprehensive Energy Systems*, 1st ed; Dincer, I., Ed.; Elsevier: 2018; pp 265−339.

(31) Kutner, M. H.; Nachtsheim, C. J.; Neter, J.; Li, W. *Applied Linear Statistical Models*; McGraw-Hill: 2005.

(32) California Air Resource Board. *Current California GHG Emission Inventory Data*. https://ww2.arb.ca.gov/ghg-inventory-data/ (accessed 2023-05-26).

(33) California Independent System Operator. *Monthly Renewables Performance Report*; http://www.caiso.com/Documents/MonthlyRenewablesPerformanceReport-Jun2023.html (accessed 2023-07-15).

(34) Karathanos, V. T.; Belessiotis, V. G. Sun and Artificial Air Drying Kinetics of Some Agricultural Products. *J. Food Eng.* **1997**, *31* (1), 35−46.

(35) Krokida, M. K.; Karathanos, V. T.; Maroulis, Z. B.; Marinos-Kouris, D. Drying Kinetics of Some Vegetables. *J. Food Eng.* **2003**, *59* (4), 391−403.

(36) Halawa, E.; van Hoof, J.; Soebarto, V. The Impacts of the Thermal Radiation Field on Thermal Comfort, Energy Consumption, and Control—A Critical Overview. *Renewable Sustainable Energy Rev.* **2014**, *37*, 907−918.

(37) Ying, T.; Spang, E. S. Paddy Drying Technologies: A Review of Existing Literature on Energy Consumption. *Processes* **2024**, *12* (3), 532.

(38) Billiris, M. A.; Siebenmorgen, T. J. Energy Use and Efficiency of Rice-Drying Systems II. Commercial, Cross-Flow Dryer Measurements. *Appl. Eng. Agric.* **2014**, *30* (2), 217−226.

(39) *Frequently Asked Questions: How Much of U.S. Carbon Dioxide Emissions Are Associated with Electricity Generation?* https://www.eia.gov/tools/faqs/faq.php?id=427&t=3 (accessed 2023-05-15).

(40) California Energy Commission; California Public Utilities Commission; California Air Resources Board. *2021 SB 100 Joint Agency Report: Achieving 100% Clean Electricity*; California Energy Commission: Sacramento, CA, 2021. https://www.energy.ca.gov/publications/2021/2021-sb-100-joint-agency-report-achieving-100-percent-clean-electricity (accessed 2023-06-09).

https://doi.org/10.1021/acsomega.4c04153
ACS Omega 2024, 9, 38142−38152